

1 **Heritability and family-based GWAS analyses of the**
2 ***N*-acyl ethanolamine and ceramide lipidome**
3 **reveal genetic influence over circulating lipids**

4 Kathryn A. McGurk,^{1,2,*} Simon G. Williams,¹ Hui Guo,³ Hugh Watkins,^{4,5} Martin
5 Farrall,^{4,5} Heather J. Cordell,⁶ Anna Nicolaou,^{2,8} Bernard D. Keavney^{1,7,8,**}

6

7 ¹Division of Cardiovascular Sciences, Faculty of Biology, Medicine and Health,
8 Manchester Academic Health Science Centre, University of Manchester, Manchester,
9 UK

10 ²Laboratory for Lipidomics and Lipid Biology, Division of Pharmacy and Optometry,
11 Faculty of Biology, Medicine and Health, Manchester Academic Health Science
12 Centre, University of Manchester, Manchester, UK.

13 ³Division of Population Health, Health Services Research & Primary Care, Faculty of
14 Biology, Medicine and Health, Manchester Academic Health Science Centre,
15 University of Manchester, UK

16 ⁴Division of Cardiovascular Medicine, Radcliffe Department of Medicine, University
17 of Oxford, Oxford, UK

18 ⁵Wellcome Centre for Human Genetics, University of Oxford, Oxford, UK

19 ⁶Institute of Genetic Medicine, Newcastle University, Newcastle upon Tyne, UK

20 ⁷Manchester Heart Centre, Manchester University NHS Foundation Trust, UK

21 ⁸These authors contributed equally to this work

22

23

24 **Email addresses:**

25

26 Kathryn A. McGurk: Kathryn.McGurk@manchester.ac.uk

27 Simon G. Williams: simon.williams2@manchester.ac.uk

28 Hui Guo: hui.guo@manchester.ac.uk

29 Hugh Watkins: hugh.watkins@rdm.ox.ac.uk

30 Martin Farrall: mfarrall@well.ox.ac.uk

31 Heather J. Cordell: heather.cordell@newcastle.ac.uk

32 Anna Nicolaou: Anna.Nicolaou@manchester.ac.uk

33 Bernard D. Keavney: Bernard.Keavney@manchester.ac.uk

34

35

36

37

38

39

40

41 **Correspondence:**

42 *kathryn.mcgurk@manchester.ac.uk @KathrynMcGurk

43 **bernard.keavney@manchester.ac.uk @KeavneyLab

44 **Abstract**

45 Certain signalling lipids of the *N*-acyl ethanolamine (NAE) and ceramide (CER)
46 classes are emerging as novel biomarkers of cardiovascular disease. We sought to
47 establish the heritability of plasma NAEs (including endocannabinoid anandamide)
48 and CERs, and identify common DNA variants influencing the circulating
49 concentrations of the heritable lipid species. Eleven NAEs and thirty CERs were
50 analysed in plasma samples from 999 members of 196 British Caucasian families,
51 using targeted mass spectrometry-based lipidomics (UPLC-MS/MS). Family-based
52 heritability was estimated and GWAS analyses were undertaken. All lipids were
53 significantly heritable over a wide range ($h^2 = 18\%-87\%$). A missense variant
54 (rs324420) in the gene encoding the enzyme fatty acid amide hydrolase (*FAAH*),
55 which degrades NAEs, associated at GWAS significance ($P < 5 \times 10^{-8}$) with four NAEs
56 (DHEA, PEA, LEA, VEA). This SNP, previously reported to be associated with
57 addictive behaviour, was associated with an approximately 10% per-allele difference
58 in mean plasma NAE species. Additionally, we have extended the previously
59 described association between rs680379 in the gene encoding the rate limiting step of
60 CER biosynthesis (*SPTLC3*) and CERs to a wider range of species (e.g.
61 CER[N(24)S(19)] and rs680379 ($P = 4.82 \times 10^{-27}$)). We have shown three novel
62 associations (*CD83*, *SGPPI*, *FBXO28-DEGS1*) influencing plasma CER traits, two of
63 which (*SGPPI* and *DEGS1*) implicate CER species in haematological phenotypes.
64 This first genetic analysis of plasma NAE species, and a wide range of CER
65 mediators, highlights these bioactive lipids as substantially heritable and influenced
66 by SNPs in key metabolic enzymes.

67 **Introduction**

68

69 Genetic studies in large numbers of individuals have identified loci where common
70 genetic variation influences the prevalence of the major plasma lipid species, such as
71 HDL- and LDL-cholesterol, and triglycerides^{1,2}. Although lipids are not DNA-
72 encoded, their activities and metabolism are strongly controlled by DNA-encoded
73 enzymes and other proteins. Recent advances in targeted bioanalytics have enabled
74 quantitative analyses of a greater proportion of the mediator lipidome in blood,
75 supporting attempts to identify genetic associations for low-concentration bioactive
76 lipid species to potentially find disease biomarkers.

77

78 Bioactive lipids of the *N*-acyl ethanolamine (NAE) and ceramide (CER) classes have
79 potent roles in inflammation and immunity³⁻⁵. NAEs are fatty acid derivatives,
80 derived from membrane phospholipids and degraded by the enzyme fatty acid amide
81 hydrolase (*FAAH*; Figure 1A). This class of bioactive lipids includes the
82 endocannabinoid anandamide (AEA), the nuclear factor agonist palmitoyl
83 ethanolamide (PEA) and a number of other species with roles in neuronal signalling,
84 pain and obesity⁶⁻⁹. The contribution of genetic factors to the variation in NAEs has
85 not yet been studied.

86

87 Ceramides are derivatives of sphingoid bases (e.g. sphingosine and
88 dihydrosphingosine) and fatty acids (Figure 1B). The first and rate limiting step¹⁰ of
89 the *de novo* biosynthesis is catalysed by the enzyme serine palmitoyltransferase, a
90 heterodimeric protein whose monomers are encoded by the *SPTLC1-3* genes. CER
91 play important roles in apoptosis¹¹. Recently, some circulating CER derivatives of 18-

92 carbon sphingosine and non-hydroxy fatty acids (e.g. CER[N(16)S(18)]) have been
93 identified as novel biomarkers of cardiovascular death¹², type-2 diabetes, and insulin
94 resistance¹³. However, the contribution of genetic factors to the circulating levels of
95 CER has only been investigated for six species, namely: CER[N(16)S(18)],
96 CER[N(20)S(18)], CER[N(22)S(18)], CER[N(23)S(18)], CER[N(24)S(18)], and
97 CER[N(24:1)S(18)], found in plasma and serum via untargeted shotgun
98 lipidomics^{14,15}.

99

100 In this study we investigate the role of genetics in determining plasma levels of 11
101 NAE and 30 CER species, in 196 British Caucasian families comprising 999
102 individuals. Using targeted, quantitative lipidomics, we show for the first time that
103 these bioactive lipid mediators are substantially heritable, and demonstrate that
104 plasma NAEs and a wide range of CERs are influenced by SNPs in key metabolic
105 enzymes (*FAAH*, *SPTLC3*, *DEGSI*, *SGPPI*). Furthermore, we identify a novel
106 inflammatory locus (*CD83*) associated with CER species, and implicate CERs in
107 haematological phenotypes through *DEGSI* and *SGPPI*.

108 **Subjects and Methods**

109

110 *Family recruitment*

111 Families were recruited for a quantitative genetic study of hypertension and other
112 cardiovascular risk factors, and selected via a proband with essential hypertension
113 (secondary hypertension was excluded using standard clinical criteria)¹⁶. Probands
114 were recruited from outpatients attending the John Radcliffe Hospital, Oxford
115 hypertension clinic, or via their family doctors. Included family members were U.K.
116 residents of self-reported European ancestry and were required to consist of 3 or more
117 siblings quantitatively assessable for blood pressure if one parent of the sibship was
118 available for blood sampling, or 4 or more siblings if no parent was available. First,
119 second and third degree relatives were then recruited to assemble a series of extended
120 families. The collection protocol obtained ethical clearance from the Central Oxford
121 Research Ethics Committee (06/Q1605/113) and it corresponds with the principles of
122 the Declaration of Helsinki. Written informed consent was obtained from all
123 participants.

124

125 This cohort of extended families has previously been shown to have adequate power
126 to detect moderate-sized genetic influences on quantitative traits^{17,18}. The participants
127 were fully phenotyped for cardiovascular risk factors, blood biochemical measures,
128 and anthropometric traits. Non-fasting blood samples were collected, plasma
129 separated, and stored at -80°C. DNA was extracted from whole blood by standard
130 methods.

131

132

133 *UPLC/ESI-MS/MS mediator lipidomics*

134 Plasma samples were extracted and analysed by mass spectrometry as previously
135 described^{19,20}. Briefly, lipids were extracted from plasma (1 mL) using chloroform-
136 methanol in the presence of class specific internal standards: C17S, C17DS, and
137 CER[N(25)S(18)] (50 pmol/sample; Ceramide/Sphingoid Internal Standard Mixture I,
138 Avanti Polar Lipids, USA) for CER, and AEA-*d*8 (20 ng/sample; Cayman Chemical
139 Co., USA) for NAE. Targeted lipidomics was performed on a triple quadrupole mass
140 spectrometer (Xevo TQS, Waters, UK) with an electrospray ionisation probe coupled
141 to a UPLC pump (Acquity UPLC, Waters, UK). CER species were separated on a C8
142 column (2.1 x 100 mm) and NAE were separated on a C18 column (2.1 x 50 mm)
143 (both Acquity UPLC BEH, 1.7µm, Waters, UK). NAE species were quantified using
144 calibration lines of synthetic standards (Cayman Chemical); relative quantitation of
145 CER was based on class specific internal standards (Avanti Polar Lipids). Pooled
146 plasma samples from healthy volunteers were used to create quality control samples
147 that were extracted and analysed blindly alongside the familial samples.

148

149 **Statistical analysis**

150 *Covariate adjustment*

151 Systematic error was considered from a variety of sources and assessed for
152 collinearity; mass spectrometry batch and a trait created to adjust for sample
153 abnormality (haemolysis or presence of white blood cells; present in 14% of samples)
154 were included as potential covariates. Ascertainment selection was modelled via
155 binary hypertension status. The resulting concentrations for each lipid species from
156 the pooled quality control samples were used for adjustment of systematic errors
157 during extraction, quantitation, and data processing. The final set of potential

158 covariates included mass spectrometry batch, sample abnormality, quality control
159 sample measures, age, age², sex, hypertension status, BMI, and total cholesterol. The
160 lipid measurements were assessed for effect of potential covariates using stepwise
161 multiple linear regression to identify the best set of predictors, using the ‘caret’
162 package and ‘leapSeq’ method in R (version 3.5.2) (see Table S1 for predictors).
163 Multiple linear regression of the best predictors was undertaken using the ‘lm’
164 function in R. Residuals from the covariate-adjusted regression models were
165 standardized to have a mean of 0 and a variance of 1. Outliers were assessed using the
166 R package ‘car’, assessing each observation by testing them as a mean-shift outlier
167 based on studentized residuals, to remove the most extreme observations (Bonferroni
168 P-value of P<0.05). Missing values were coded as such in the genetics analyses. As
169 lipid mediators can exert individual bioactivities, all lipid species were treated
170 uniquely for all analyses, intra-class correlation analyses are depicted in Figure S1.

171

172 *Genome-wide genotyping quality control*

173 Genotyping was performed using the Illumina 660W-Quad chip on 1,234 individuals
174 (580 males and 654 females) including 248 founders, at 557,124 SNPs. Quality
175 control of the genotyping data was undertaken using PLINK²¹ (version 1.9). No
176 duplicate variants were found. SNPs that were identified as Mendelian inconsistencies
177 (--mendel-multigen) were marked as missing. Gender checks assessed by F-statistic
178 (--check-sex) showed that gender as inferred from 538,771 chromosomal SNPs
179 agreed with reported status. SNPs with low genotyping rates (--geno 0.05), low minor
180 allele frequency (--maf 0.01), and those that failed checks of Hardy-Weinberg
181 Equilibrium (--hwe 1e-8) were excluded. Individuals with low genotype rates (--mind
182 0.05) and outlying heterozygosity were removed (0.31 - 0.33 included). Relatedness

183 was assessed by high levels of IBD sharing (--genome and --rel-check) and by
184 visualisation of pairs of individuals' degree of relatedness (through plotting the
185 proportion of loci where the pair shares one allele IBD (Z1) by the proportion of loci
186 where the pair shares zero alleles IBD (Z0)), and two outlier individuals were
187 removed. Ethnicity was assessed via principal components analysis with genotype
188 data from the 1,000 Genome Project²², which confirmed all participants were of
189 European/CEU origin. Following quality control, 503,221 autosomal SNPs from
190 1,219 individuals (216 families) were available for SNP-based heritability
191 assessments, of which 999 individuals (196 families; 198 founders and 801 non-
192 founders) had plasma available for lipidomics.

193

194 *Heritability estimates*

195 SNP-based heritability was estimated using GCTA software (version 1.26.0)^{23,24}. A
196 genetic relationship matrix was created from the quality controlled genotyping data
197 and the --reml command was used to estimate variance of the traits explained by the
198 genotyped SNPs. A complementary estimation of pedigree-based heritability was
199 undertaken using the QTDT software (version 2.6.1)²⁵, by specifying the -we and -veg
200 options to compare an environmental only variance model with a polygenic and
201 environmental variances model. The P-values presented are adjusted for 30 tests
202 (CER) or 11 tests (NAE) via Bonferonni correction. The least significant adjusted P-
203 value from the groups of lipid species described are depicted as $P_{adj} < X$.

204

205 *Genotyping imputation*

206 Following genotyping quality control, 503,221 autosomal SNPs were available to
207 inform imputation. Imputation was performed through the Michigan Imputation

208 Server (version v1.0.4)²⁶, specifying pre-phasing with Eagle²⁷ (version 2.3) and
209 imputation by Minimac3²⁶ using the European population of the Human Reference
210 Consortium²⁸ (version hrc.r1.1.2016). Following imputation, duplicate SNPs and
211 SNPs with $r^2 < 0.8$ were removed to generate a final set of 10,652,600 SNPs. Quality
212 control was undertaken for the imputed data on the 999 individuals with lipidomics
213 available, as follows: SNPs that were identified as Mendelian inconsistencies (--
214 mendel-multigen) were marked as missing. SNPs with low call rates (--geno 0.05),
215 low minor allele frequency (--maf 0.05), and those that failed checks of Hardy-
216 Weinberg Equilibrium (--hwe 1e-8) were excluded, resulting in a final count of
217 5,280,459 SNPs available for genome-wide association analyses.

218

219 *Family-based genome-wide association studies*

220 Linear mixed modelling approaches were used to account for family structure.
221 Family-based genome-wide association analyses were undertaken for each lipid trait
222 using GCTA software (version 1.26.0), specifying mixed linear model association
223 analyses (--mlma). Genomic control inflation factors from the GWAS analyses can be
224 found in Table S2. The least significant P-values of the significantly associated SNPs
225 ($P < 5 \times 10^{-8}$) are depicted as P<X in the manuscript. Significantly associated SNPs were
226 analysed by Ensembl API Client (version 1.1.5 on GRCh37.p13) to identify
227 neighbouring genes. Further analyses were undertaken of the significantly associated
228 SNPs; expression quantitative trait loci (eQTL) were identified using the GTEx portal
229 browser (version 8), assessment of previously identified SNPs from GWAS was
230 undertaken using the GWAS Catalog, and assessment of PheWAS with the UK
231 Biobank²⁹ was undertaken using the Gene Atlas Browser (see Web Resources).

232

233 *Two-sample Mendelian randomisation analysis*

234 Two sample Mendelian randomisation (2SMR) analysis was undertaken in R
235 following the guidelines provided by Davey Smith et al
236 [<https://mrcieu.github.io/TwoSampleMR/>]³⁰. Briefly, selected examples of the
237 significant associations identified for each class of lipid were analysed by 2SMR for a
238 number of previously published GWAS of interest. The GWAS significant
239 associations ($P < 5 \times 10^{-8}$) identified for NAE species PEA, and CER traits
240 CER[N(22)S(19)], CER[N(24)S(16)], and CER[N(24)S(19)]/CER[N(24)DS(19)]
241 ratio, were assessed for coronary artery disease (all), addiction (PEA), Type-2
242 Diabetes (CER[N(22)S(19)]), and blood cell counts (CER[N(24)S(16)] and
243 CER[N(24)S(19)]/CER[N(24)DS(19)] ratio). Details on the published GWAS used as
244 outcomes are presented in Table S3. As many GWAS associated SNPs were in
245 linkage disequilibrium, the following SNPs remained in the analysis after the data
246 clumping step; rs324420 (*FAAH*; PEA), rs438568 (*SPTLC3*; CER[N(22)S(19)]),
247 rs7160525 (*SGPPI1*; CER[N(24)S(16)]), and rs4653568 (*DEGS1*; CER[N(24)S(19)]/
248 CER[N(24)DS(19)] ratio).

249 **Results**

250 *Population characteristics*

251 Plasma samples of 999 participants from 196 British Caucasian families were
252 included in the genetic analyses. The families consisted of 1-24 members (mean of 5
253 members) with plasma available for lipidomics analyses (Figure S2). Participant
254 descriptions are listed in Table 1.

255

256 *Lipidomics descriptive statistics*

257 Of the 11 NAE species identified in plasma, palmitoyl ethanolamide (PEA) was at
258 highest abundance (1.89 ± 1.36 ng/ml (mean \pm SD)), and of the 30 plasma CER
259 species, CER[N(24)S(18)] was most abundant (128.87 ± 61.00 pmol/ml). In some
260 cases, the ratio of product/precursor metabolites involved in specific enzymatic
261 reactions was measured; this allowed for examination of the genetic variants in
262 corresponding enzymes (e.g. the ratio CER[NS] to CER[NDS] is indicative of *DEGSI*
263 activity, Figure 1B). Structure-based summations of total abundance and ratios that
264 have previously been associated in the literature with cardiovascular risk¹² were also
265 assessed for genetic associations. A list of the species and measurements studied, and
266 summary statistics are presented in Table S4.

267

268 *Signalling lipid species are highly heritable*

269 The NAE species had estimated heritabilities ranging from 45% to 82%
270 ($P_{\text{adj}} < 6.72 \times 10^{-15}$), with pentadecanoyl ethanolamide (PDEA) having the highest
271 estimated heritability. Ceramide species showed a wide range in estimated
272 heritability. Of the CER classes examined, CER[NS] species had heritabilities
273 between 18% - 62% ($P_{\text{adj}} < 4.50 \times 10^{-2}$), CER[NDS] species had estimated heritability of

274 32% - 52%, ($P_{\text{adj}} < 3.00 \times 10^{-11}$), while CER[AS], sphingosine-1-phosphate (C18S1P),
275 sphingosine (C18S) and dihydrosphingosine (C18DS) were all significantly heritable.
276 Heritability results are depicted in Figure 2 (a detailed list is provided in Table S5).

277

278 *Genome-wide association study of N-acyl ethanolamines*

279 There were conventionally GWAS significant ($P < 5 \times 10^{-8}$) associations between four
280 NAEs (N-docosahexaenoyl ethanolamide, DHEA; N-linoleoyl ethanolamide, LEA;
281 N-palmitoyl ethanolamide PEA; vaccinoyl ethanolamide, VEA), as well as the sum of
282 all NAEs (sumEA), with SNPs in the gene encoding fatty acid amide hydrolase
283 (*FAAH*; Figure 3, with details in Table S6), which catalyses the degradation of NAEs
284 (Figure 1A). The leading SNP is a missense variant (rs324420; C385A; P129T) and
285 eQTL of *FAAH* in multiple tissues including whole blood. Presence of the missense
286 variant causes the enzyme to display normal catalytic properties but decreased cellular
287 stability³¹ by enhanced sensitivity of the enzyme to proteolytic degradation³². The
288 magnitude of the genetic effect was considerable; for example, participants with the
289 AA genotype of the lead SNP rs324420 had 22% increased mean plasma
290 concentration of PEA (2.19 ± 1.57 ng/ml, n=51) compared to those carrying the CC
291 genotype (1.79 ± 1.29 ng/ml, n=639). A LocusZoom plot of the association with the
292 lipid PEA is depicted in Figure 4, with the 22-chromosome Manhattan plot depicted
293 in Figure S3.

294

295 *Genome-wide association study of ceramides and related sphingolipids*

296 Seven CER[NS] and two CER[NDS] species were significantly associated with SNPs
297 in an intergenic region on chromosome 20 (Figure 5, with example Manhattan plot
298 depicted in Figure S4, and further details in Table S7). Assessing the SNPs using

299 GTE_x confirmed them as liver eQTLs (Table S8) found 20,000 bases downstream of
300 the gene encoding the third subunit of serine palmitoyltransferase (*SPTLC3*; Figure
301 6), which catalyses the rate-limiting step¹⁰ of CER biosynthesis (Figure 1B). The
302 SNPs are associated with differences in the expression of the *SPTLC3* gene in the
303 liver, leading to changes in CER production that are reflected in altered plasma levels.
304 Associated SNPs had considerable phenotypic effects, for example the AA genotype
305 of the SNP rs680379 was associated with a 48% increase in the concentration of
306 CER[N(24)S(19)] compared with the GG genotype (62.84 ± 24.86 pmol/ml [n=148],
307 and 42.44 ± 18.48 pmol/ml [n=409], respectively). Furthermore, the summed total of
308 all CER species with 24-carbon non-hydroxy fatty acids, and, independently, those
309 with 19- and 20-carbon sphingosine bases, were found associated with the same SNPs
310 at the *SPTLC3* locus (Table S8). A novel association was identified for
311 CER[N(26)S(19)] at a locus on chromosome 6, upstream to the gene for inflammatory
312 protein CD83 (e.g. rs6940658, $P=2.07 \times 10^{-8}$; depicted in Figure S5 with further details
313 in Table S7).

314

315 *Association of ceramides and related traits with hematological phenotypes*

316 The Gene Atlas Browser of PheWAS in the UK Biobank study was used to assess the
317 association of significant SNPs identified here with the extensive number of
318 phenotypes measured for the UK Biobank cohort. The ratio of CER[NS] to their
319 precursor CER[NDS], is indicative of delta 4-desaturase, sphingolipid 1 (*DEGSI*)
320 activity (Figure 1B). A set of SNPs in the upstream region of the *DEGSI* gene on
321 chromosome 1 associated with the product/precursor ratio,
322 CER[N(24)S(19)]/CER[N(24)DS(19)] ($P=4.34 \times 10^{-8}$; depicted in Figure S6 with
323 further details in Table S7). All significant SNPs were confirmed eQTLs of *DEGSI* in

324 whole blood (Table S8). This locus associated with numerous blood cell phenotypes
325 in the UKBiobank data (e.g. rs4653568 and mean platelet (thrombocyte) volume;
326 $P=4.77 \times 10^{-12}$; Table S8). A further set of SNPs upstream of the gene encoding
327 sphingosine-1 phosphate phosphatase (*SGPPI*) were associated with
328 CER[N(24)S(16)] (e.g. rs7160525, $P=5.67 \times 10^{-10}$; Figure S7). This enzyme is involved
329 in the recycling of CER[NS] species from sphingosine-1-phosphate and ceramide-1-
330 phosphate (C1P) (Figure 1B). All significant SNPs at this locus were also associated
331 with blood cell phenotypes, identified in the UK Biobank data (e.g. rs7160525 and
332 mean platelet (thrombocyte) volume, $P=3.28 \times 10^{-29}$; Table S8). The significant SNPs
333 identified at both *SGPPI* and *DEGSI* were assessed by 2SMR using published blood
334 cell count GWAS as outcome variables. The SNPs at both loci were found significant
335 using 2SMR ($P < 0.05$) in influencing platelet, red blood cell, and white blood cell
336 traits. Table S9 describes the results in detail.

337

338 No significant GWAS associations were found with the particular CER species that
339 have been previously investigated as biomarkers of coronary artery disease and type-2
340 diabetes (e.g. CER[N(16)S(18)]). The *SPTLC3* locus has associated with these CERs
341 previously. Therefore, an example CER (CER[N(22)S(19)]) which associated at
342 GWAS significantly with the *SPTLC3* locus was used to investigate the causality via
343 two-sample Mendelian randomisation between the identified SNPs in *SPTLC3* with
344 coronary artery disease and type-2 diabetes. There was no significant association
345 between the *SPTLC3* locus and the cardiovascular disease endpoints (Table S9).

346 **Discussion**

347 We show, for the first time, the substantial variation in heritability estimated for an
348 array of signalling lipid mediators found in plasma, including low concentration
349 members of the NAE and CER classes, and we identify GWAS significant
350 associations between lipids and variants of the enzymes in their respective metabolic
351 pathways. We have provided the first GWAS significant evidence of association
352 between SNPs in the *FAAH* gene and plasma NAEs. Additionally, we have extended
353 the previously described association between SNPs in the *SPTLC3* gene and plasma
354 CERs to a wider range of species. Our results indicate that these two genes are the
355 major loci influencing plasma levels of NAEs and CERs, respectively. In addition, we
356 have shown novel SNP associations (*CD83*, *SGPPI*, *FBXO28-DEGS1*) influencing
357 plasma CER species.

358

359 *Genetic analyses of N-acyl ethanolamine species*

360 We show for the first time associations at GWAS significance for NAE species
361 (DHEA, LEA, PEA, and VEA) with a missense change in the NAE degradation
362 enzyme FAAH. The association with PEA was identified previously in a single
363 candidate gene study of mutations in *FAAH* in 114 subjects³³, which reported the
364 same direction of effect on plasma AEA, PEA, STEA and OEA species but with P-
365 values insignificant at genome-wide levels ($0.003 < P < 0.04$). Here, in this study of 999
366 related participants, we identified additional NAE species significantly associated
367 with the SNP (DHEA, LEA, and VEA), though we did not find significant association
368 at the locus for AEA, STEA or OEA species. We observed a similar trend to the
369 previous paper when comparing the plasma levels of NAE species between

370 participants with the missense AA genotype, and those with the wildtype CC
371 genotype (Figure S8).

372

373 While the *FAAH* missense SNP rs324420 is not associated with any disease endpoints
374 identified from GWAS to date, the A allele, associated with higher NAE levels, has
375 been reported to increase the risk of polysubstance addiction and abuse [MIM:
376 606581] in three candidate gene studies totaling 863 cases and 2,170 controls^{32,34,35}
377 and to potentially contribute to pain insensitivity³⁶ [MIM: 618377], obesity³⁷, and
378 anxiety^{38,39}. PheWAS analysis using the Gene Atlas UK Biobank online browser
379 however did not identify significant association in a similar number of UK Biobank
380 cases of substance abuse/dependency (OR for A allele = 1.10; P = 0.14; 746 cases and
381 451,518 controls) nor the further 2SMR analyses undertaken here using UK Biobank
382 addiction treatment codes (18 cases, 462999 controls; Table S9). It is possible that
383 misclassification bias has affected the UK Biobank PheWAS; among the 451,518 UK
384 Biobank participants assigned as controls, some reported dependencies on other
385 substances and behaviours, such as coffee, cigarettes, prescription drugs, and
386 gambling. The potential implication of NAE species in addiction through the
387 association with the *FAAH* SNP, warrants further investigation in larger numbers of
388 cases.

389

390 As direct cannabinoid receptor 1 (CB1) antagonist drugs have caused severe adverse
391 psychiatric effects⁴⁰, *FAAH* inhibitors are being evaluated as an alternative approach
392 to modulating endocannabinoid signalling. However, in 2016, a *FAAH* inhibitor
393 resulted in severe neurological side-effects in a Phase I trial, hypothesised due to off-
394 target drug effects⁴¹. As the functional *FAAH* SNP rs324420 did not associate with

395 any adverse phenotypes in the UK Biobank, it is likely that on-target effects of FAAH
396 inhibitor drugs do not have substantial risks of causing conditions that occurred with
397 appreciable frequency in UK Biobank.

398

399 *Genetic analyses of ceramides and other sphingolipid species*

400 Narrow-sense heritability has been estimated for six CER (CER[N(16)S(18)],
401 CER[N(18)S(18)], CER[N(20)S(18)], CER[N(22)S(18)], CER[N(24)S(18)],
402 CER[N(24:1)S(18)] and the corresponding dihydroceramide species
403 (CER[N(16)DS(18)], CER[N(18)DS(18)], CER[N(20)DS(18)], CER[N(22)DS(18)],
404 CER[N(24)DS(18)], CER[N(24:1)DS(18)], showing estimated heritability of 0.37 -
405 0.51 ($P < 0.01$) for CER[NS] and 0.09 - 0.34 ($P < 0.01$) for CER[NDS] in 42 Mexican
406 American families⁴². Here, we show assessing a larger array of species, that further
407 CER[NS] and CER[NDS] were significantly heritable, expanding on these previous
408 estimates.

409

410 The rs7157785 variant in sphingosine 1-phosphate phosphatase 1 (*SGPPI*), a CER
411 metabolic enzyme, has been identified previously in GWAS of sphingomyelin^{14,15,43},
412 total cholesterol⁴⁴, glycerophospholipids⁴³, total cholesterol⁴⁴, and the ratio of an
413 unknown blood lipid (X-08402) to cholesterol⁴⁵. The novel association with
414 CER[N(24)S(16)] we describe is consistent with the gene's role in influencing
415 CER[NS] production, through the formation of sphingosine (C18S) for CER[NS]
416 biosynthesis, and the production of CER[NS] from ceramide 1-phosphate (C1P)
417 (Figure 1). The other significant SNPs identified at the same locus which associated
418 with this CER species have been previously identified in further GWAS studies of
419 blood phospholipids⁴⁶, red cell distribution width⁴⁷, sphingomyelin⁴⁶, and unknown

420 blood metabolite X-10510⁴⁵. All SNPs identified at this locus associated in the
421 UKBiobank PheWAS assessment, and 2SMR analyses, with multiple blood cell
422 counts and other hematological phenotypes (Table S8). Association with
423 hematological phenotypes was also identified for the locus on chromosome 1 at
424 *DEGSI*, found via the GWAS results analysing the ratio of CER[N(24)S(19)] to
425 CER[N(24)DS(19)]. CER have been previously shown to stimulate erythrocyte
426 formation through platelet activating factor⁴⁸. However, further studies will be
427 required to identify the mechanism of the association between genetically determined
428 plasma ceramide levels and blood cell phenotypes.

429

430 CER[N(26)S(19)] associated at GWAS with SNPs at a novel locus on chromosome 6,
431 upstream to the gene encoding the inflammatory protein CD83 ($P=2.07 \times 10^{-8}$), a
432 member of the immunoglobulin superfamily of membrane receptors expressed by
433 antigen-presenting white blood cells, leukocytes, and dendritic cells⁴⁹. An interaction
434 between CD83 and CER is currently unknown, but given the involvement of ceramide
435 signalling in inflammation and immunity^{50,51}, it would be of interest to investigate
436 further.

437

438 Association between some CER species and the *SPTLC3* SNP rs680379 has been
439 identified previously through the use of shotgun lipidomics for five CER species
440 (CER[N(16)S(18)], CER[N(22)S(18)], CER[N(23)S(18)], CER[N(24)S(18)], and
441 CER[N(24:1)S(18)])^{14,15}. Here, we identify associations between an additional seven
442 CER[NS] and two CER[NDS] plasma species and this SNP, and with other eQTLs of
443 serine palmitoyltransferase at the same locus; as this enzyme is the rate limiting step
444 for the *de novo* biosynthesis of CER, this association may have wider implications.

445 The information gathered from the eQTL analysis highlights all of the *SPTLC3*
446 confirmed eQTLs act in the liver, which is a major site for plasma CER biosynthesis.
447 PheWAS analysis in UK Biobank, nor 2SMR analysis, did not identify significant
448 disease associations with the *SPTLC3* locus. A number of CER[NS] species have
449 been studied as potential biomarkers of cardiovascular disease and diabetes^{12,52}. While
450 GWAS significant associations were not found with these lipids, the extent to which
451 specific species have a role in cardiovascular disease remains debated⁵³⁻⁶⁰.

452

453 The sample size analysed here (999 participants) is the largest study analysing this
454 number of plasma NAE and CER species to date⁶¹. However, it is still a modest study
455 for GWAS analyses. The associations we have uncovered suggest that further
456 investigation of heritable lipid species for which no GWAS association was found in
457 this study would be of interest.

458 **Supplemental Data**

459 Supplemental Data include nine tables and eight figures.

460

461 **Acknowledgements**

462 We are very grateful to the families involved in this study. K.M. is supported by an

463 MRC Doctoral Award (MR/K501311/1), the University of Manchester President's

464 Doctoral Scholarship, and Doctoral Academy Society Membership Fund. AN is

465 supported in part by the NIHR Manchester Biomedical Research Centre. BK is

466 supported by a BHF Personal Chair.

467

468 **Declaration of interests**

469 The authors declare no competing interests.

470

471 **Web Resources**

472 OMIM: <http://www.omim.org/>

473 GWAS Catalog: <https://www.ebi.ac.uk/gwas/>

474 GTEx Portal: <https://gtexportal.org/>

475 UCSC Genome Browser: <https://genome.ucsc.edu/cgi-bin/hgGateway/>

476 Gene Atlas UKBiobank Browser: <http://geneatlas.roslin.ed.ac.uk/>

477 UKBiobank Data Show case [April 2019]: <http://biobank.ndph.ox.ac.uk/showcase/>

478 LocusZoom: <http://csg.sph.umich.edu/locuszoom/>

479 **References**

- 480 1. Teslovich, T.M., Musunuru, K., Smith, A. V, Edmondson, A.C., Stylianou, I.M.,
481 Koseki, M., Pirruccello, J.P., Ripatti, S., Chasman, D.I., Willer, C.J., et al. (2010).
482 Biological, clinical and population relevance of 95 loci for blood lipids. *Nature* 466,
483 707–713.
- 484 2. Willer, C.J., Schmidt, E.M., Sengupta, S., Peloso, G.M., Gustafsson, S., Kanoni, S.,
485 Ganna, A., Chen, J., Buchkovich, M.L., Mora, S., et al. (2013). Discovery and
486 refinement of loci associated with lipid levels. *Nat. Genet.* 45, 1274–1285.
- 487 3. MacEyka, M., and Spiegel, S. (2014). Sphingolipid metabolites in inflammatory
488 disease. *Nature* 510, 58–67.
- 489 4. Kendall, A.C., and Nicolaou, A. (2013). Bioactive lipid mediators in skin
490 inflammation and immunity. *Prog. Lipid Res.* 52, 141–164.
- 491 5. Sugamura, K., Sugiyama, S., Nozaki, T., Matsuzawa, Y., Izumiya, Y., Miyata, K.,
492 Nakayama, M., Kaikita, K., Obata, T., Takeya, M., et al. (2009). Activated
493 endocannabinoid system in coronary artery disease and anti inflammatory effects of
494 cannabinoid 1 receptor blockade on macrophages. *Circulation* 119, 28–36.
- 495 6. Devane, W.A., Hanuš, L., Breuer, A., Pertwee, R.G., Stevenson, L.A., Griffin, G.,
496 Gibson, D., Mandelbaum, A., Etinger, A., and Mechoulam, R. (1992). Isolation and
497 structure of a brain constituent that binds to the cannabinoid receptor. *Science* (80-.).
498 258, 1946–1949.
- 499 7. Wilson, R.I., and Nicoll, R. a (2001). Endogenous cannabinoids mediate retrograde
500 signalling at hippocampal synapses. *Nature* 410, 588–592.
- 501 8. Hohmann, A.G., Suplita, R.L., Bolton, N.M., Neely, M.H., Fegley, D., Mangieri,
502 R., Krey, J.F., Michael Walker, J., Holmes, P. V., Crystal, J.D., et al. (2005). An
503 endocannabinoid mechanism for stress-induced analgesia. *Nature* 435, 1108–1112.

- 504 9. Engeli, S., Böhnke, J., Feldpausch, M., Gorzelniak, K., Janke, J., Bátkai, S., Pacher,
505 P., Harvey-White, J., Luft, F.C., Sharma, A.M., et al. (2005). Activation of the
506 peripheral endocannabinoid system in human obesity. *Diabetes* 54, 2838–2843.
- 507 10. Perry, D.K., Carton, J., Shah, A.K., Meredith, F., Uhlinger, D.J., and Hannun,
508 Y.A. (2000). Serine palmitoyltransferase regulates de novo ceramide generation
509 during etoposide-induced apoptosis. *J. Biol. Chem.* 275, 9078–9084.
- 510 11. Perry, D.K., and Hannun, Y.A. (1998). The role of ceramide in cell signaling.
511 *Biochim. Biophys. Acta* 1436, 233–243.
- 512 12. Laaksonen, R., Ekroos, K., Sysi-Aho, M., Hilvo, M., Vihervaara, T., Kauhanen,
513 D., Suoniemi, M., Hurme, R., März, W., Scharnagl, H., et al. (2016). Plasma
514 ceramides predict cardiovascular death in patients with stable coronary artery disease
515 and acute coronary syndromes beyond LDL-cholesterol. *Eur. Heart J.* 37, 1967–1976.
- 516 13. Haus, J.M., Kashyap, S.R., Kasumov, T., Zhang, R., Kelly, K.R., Defronzo, R.A.,
517 and Kirwan, J.P. (2009). Plasma ceramides are elevated in obese subjects with type 2
518 diabetes and correlate with the severity of insulin resistance. *Diabetes* 58, 337–343.
- 519 14. Hicks, A.A., Pramstaller, P.P., Johansson, A., Vitart, V., Rudan, I., Ugocsai, P.,
520 Aulchenko, Y., Franklin, C.S., Liebisch, G., Erdmann, J., et al. (2009). Genetic
521 determinants of circulating sphingolipid concentrations in European populations.
522 *PLoS Genet.* 5, e1000672.
- 523 15. Demirkan, A., van Duijn, C.M., Ugocsai, P., Isaacs, A., Pramstaller, P.P.,
524 Liebisch, G., Wilson, J.F., Johansson, Å., Rudan, I., Aulchenko, Y.S., et al. (2012).
525 Genome-wide association study identifies novel loci associated with circulating
526 phospho- and sphingolipid concentrations. *PLoS Genet.* 8, e1002490.
- 527 16. Keavney, B., Mayosi, B., Gaukrodger, N., Imrie, H., Baker, M., Fraser, R.,
528 Ingram, M., Watkins, H., Farrall, M., Davies, E., et al. (2005). Genetic variation at the

529 locus encompassing 11-beta hydroxylase and aldosterone synthase accounts for
530 heritability in cortisol precursor (11-deoxycortisol) urinary metabolite excretion. *J.*
531 *Clin. Endocrinol. Metab.* *90*, 1072–1077.

532 17. Baker, M., Rahman, T., Hall, D., Avery, P.J., Mayosi, B.M., Connell, J.M.C.,
533 Farrall, M., Watkins, H., and Keavney, B. (2007). The C-532T polymorphism of the
534 angiotensinogen gene is associated with pulse pressure: A possible explanation for
535 heterogeneity in genetic association studies of AGT and hypertension. *Int. J.*
536 *Epidemiol.* *36*, 1356–1362.

537 18. Vickers, M.A., Green, F.R., Terry, C., Mayosi, B.M., Julier, C., Lathrop, M.,
538 Ratcliffe, P.J., Watkins, H.C., and Keavney, B. (2002). Genotype at a promoter
539 polymorphism of the interleukin-6 gene is associated with baseline levels of plasma
540 C-reactive protein. *Cardiovasc. Res.* *53*, 1029–1034.

541 19. Kendall, A.C., Pilkington, S.M., Massey, K. a, Sassano, G., Rhodes, L.E., and
542 Nicolaou, A. (2015). Distribution of Bioactive Lipid Mediators in Human Skin. *J.*
543 *Invest. Dermatol.* *135*, 1510–1520.

544 20. Cucchi, D., Camacho-Muñoz, D., Certo, M., Niven, J., Smith, J., Nicolaou, A.,
545 and Mauro, C. (2019). Omega-3 polyunsaturated fatty acids impinge on CD4+ T cell
546 motility and adipose tissue distribution via direct and lipid mediator-dependent
547 effects. *Cardiovasc. Res.* *cvz208*.

548 21. Purcell, S., Neale, B., Todd-Brown, K., Thomas, L., Ferreira, M.A.R., Bender, D.,
549 Maller, J., Sklar, P., de Bakker, P.I.W., Daly, M.J., et al. (2007). PLINK: A tool set
550 for whole-genome association and population-based linkage analyses. *Am. J. Hum.*
551 *Genet.* *81*, 559–575.

552 22. Auton, A., Abecasis, G.R., Altshuler, D.M., Durbin, R.M., Bentley, D.R.,
553 Chakravarti, A., Clark, A.G., Donnelly, P., Eichler, E.E., Flicek, P., et al. (2015). A

- 554 global reference for human genetic variation. *Nature* 526, 68–74.
- 555 23. Yang, J., Benyamin, B., McEvoy, B.P., Gordon, S., Henders, A.K., Nyholt, D.R.,
556 Madden, P.A., Heath, A.C., Martin, N.G., Montgomery, G.W., et al. (2010). Common
557 SNPs explain a large proportion of the heritability for human height. *Nat. Genet.* 42,
558 565–569.
- 559 24. Zaitlen, N., Kraft, P., Patterson, N., Pasaniuc, B., Bhatia, G., Pollack, S., and
560 Price, A.L. (2013). Using Extended Genealogy to Estimate Components of
561 Heritability for 23 Quantitative and Dichotomous Traits. *PLoS Genet.* 9, e1003520.
- 562 25. Abecasis, G.R., Cardon, L.R., and Cookson, W.O. (2000). A general test of
563 association for quantitative traits in nuclear families. *Am. J. Hum. Genet.* 66, 279–
564 292.
- 565 26. Das, S., Forer, L., Schönherr, S., Sidore, C., Locke, A.E., Kwong, A., Vrieze, S.I.,
566 Chew, E.Y., Levy, S., McGue, M., et al. (2016). Next-generation genotype imputation
567 service and methods. *Nat. Genet.* 48, 1284–1287.
- 568 27. Loh, P.R., Danecek, P., Palamara, P.F., Fuchsberger, C., Reshef, Y.A., Finucane,
569 H.K., Schoenherr, S., Forer, L., McCarthy, S., Abecasis, G.R., et al. (2016).
570 Reference-based phasing using the Haplotype Reference Consortium panel. *Nat.*
571 *Genet.* 48, 1443–1448.
- 572 28. McCarthy, S., Das, S., Kretzschmar, W., Delaneau, O., Wood, A.R., Teumer, A.,
573 Kang, H.M., Fuchsberger, C., Danecek, P., Sharp, K., et al. (2016). A reference panel
574 of 64,976 haplotypes for genotype imputation. *Nat. Genet.* 48, 1279–1283.
- 575 29. Sudlow, C., Gallacher, J., Green, J., Sprosen, T., Pell, J., Burton, P., Matthews, P.,
576 Liu, B., Danesh, J., Downey, P., et al. (2015). UK Biobank: an open access resource
577 for identifying the causes of a wide range of complex diseases of middle and old Age.
578 *PLOS Med.* 12, e1001779.

- 579 30. Smith, G.D., and Hemani, G. (2014). Mendelian randomization: Genetic anchors
580 for causal inference in epidemiological studies. *Hum. Mol. Genet.* 23, R89–R98.
- 581 31. Chiang, K.P., Gerber, A.L., Sipe, J.C., and Cravatt, B.F. (2004). Reduced cellular
582 expression and activity of the P129T mutant of human fatty acid amide hydrolase:
583 Evidence for a link between defects in the endocannabinoid system and problem drug
584 use. *Hum. Mol. Genet.* 13, 2113–2119.
- 585 32. Sipe, J.C., Chiang, K., Gerber, A.L., Beutler, E., and Cravatt, B.F. (2002). A
586 missense mutation in human fatty acid amide hydrolase associated with problem drug
587 use. *Proc. Natl. Acad. Sci.* 99, 8394–8399.
- 588 33. Sipe, J.C., Scott, T.M., Murray, S., Harismendy, O., Simon, G.M., Cravatt, B.F.,
589 and Waalen, J. (2010). Biomarkers of endocannabinoid system activation in severe
590 obesity. *PLoS One* 5, 1–6.
- 591 34. Flanagan, J.M., Gerber, A.L., Cadet, J.L., Beutler, E., and Sipe, J.C. (2006). The
592 fatty acid amide hydrolase 385 A/A (P129T) variant: Haplotype analysis of an ancient
593 missense mutation and validation of risk for drug addiction. *Hum. Genet.* 120, 581–
594 588.
- 595 35. Sim, M.S., Hatim, A., Reynolds, G.P., and Mohamed, Z. (2013). Association of a
596 functional FAAH polymorphism with methamphetamine-induced symptoms and
597 dependence in a Malaysian population. *Pharmacogenomics* 14, 505–514.
- 598 36. Cajanus, K., Holmström, E.J., Wessman, M., Anttila, V., Kaunisto, M.A., and
599 Kalso, E. (2016). Effect of endocannabinoid degradation on pain: role of FAAH
600 polymorphisms in experimental and postoperative pain in women treated for breast
601 cancer. *Pain* 157, 361–369.
- 602 37. Sipe, J.C., Waalen, J., Gerber, A., and Beutler, E. (2005). Overweight and obesity
603 associated with a missense polymorphism in fatty acid amide hydrolase (FAAH). *Int.*

- 604 J. *Obes.* 29, 755–759.
- 605 38. Dincheva, I., Drysdale, A.T., Hartley, C.A., Johnson, D.C., Jing, D., King, E.C.,
606 Ra, S., Gray, J.M., Yang, R., DeGruccio, A.M., et al. (2015). FAAH genetic variation
607 enhances fronto-amygdala function in mouse and human. *Nat. Commun.* 6, 1–9.
- 608 39. Lazary, J., Eszlari, N., Juhasz, G., and Bagdy, G. (2016). Genetically reduced
609 FAAH activity may be a risk for the development of anxiety and depression in
610 persons with repetitive childhood trauma. *Eur. Neuropsychopharmacol.* 26, 1020–
611 1028.
- 612 40. Mach, F., Montecucco, F., and Steffens, S. (2009). Effect of blockage of the
613 endocannabinoid system by CB1 antagonism on cardiovascular risk. *Pharmacol.*
614 *Reports* 61, 13–21.
- 615 41. Mallet, C., Dubray, C., and Dualé, C. (2016). FAAH inhibitors in the limelight,
616 but regrettably. *Int. J. Clin. Pharmacol. Ther.* 54, 498–501.
- 617 42. Bellis, C., Kulkarni, H., Mamtani, M., Kent, J.W., Wong, G., Weir, J.M., Barlow,
618 C.K., Diego, V., Almeida, M., Dyer, T.D., et al. (2014). Human plasma lipidome is
619 pleiotropically associated with cardiovascular risk factors and death. *Circ.*
620 *Cardiovasc. Genet.* 7, 854–863.
- 621 43. Draisma, H.H.M., Pool, R., Kobl, M., Jansen, R., Petersen, A.-K., Vaarhorst,
622 A.A.M., Yet, I., Haller, T., Demirkan, A., Esko, T., et al. (2015). Genome-wide
623 association study identifies novel genetic variants contributing to variation in blood
624 metabolite levels. *Nat. Commun.* 6, 7208.
- 625 44. Klarin, D., Damrauer, S.M., Cho, K., Sun, Y. V., Teslovich, T.M., Honerlaw, J.,
626 Gagnon, D.R., DuVall, S.L., Li, J., Peloso, G.M., et al. (2018). Genetics of blood
627 lipids among ~300,000 multi-ethnic participants of the Million Veteran Program. *Nat.*
628 *Genet.* 50, 1514–1523.

- 629 45. Shin, S.Y., Fauman, E.B., Petersen, A.K., Krumsiek, J., Santos, R., Huang, J.,
630 Arnold, M., Erte, I., Forgetta, V., Yang, T.P., et al. (2014). An atlas of genetic
631 influences on human blood metabolites. *Nat. Genet.* *46*, 543–550.
- 632 46. Li, Y., Sekula, P., Wuttke, M., Wahrheit, J., Hausknecht, B., Schultheiss, U.T.,
633 Gronwald, W., Schlosser, P., Tucci, S., Ekici, A.B., et al. (2018). Genome-wide
634 association studies of metabolites in patients with CKD identify multiple loci and
635 illuminate tubular transport mechanisms. *J. Am. Soc. Nephrol.* *29*, 1513–1524.
- 636 47. Astle, W.J., Elding, H., Jiang, T., Allen, D., Ruklisa, D., Mann, A.L., Mead, D.,
637 Bouman, H., Riveros-Mckay, F., Kostadima, M.A., et al. (2016). The Allelic
638 Landscape of Human Blood Cell Trait Variation and Links to Common Complex
639 Disease. *Cell* *167*, 1415–1429.
- 640 48. Lang, P.A., Kempe, D.S., Tanneur, V., Eisele, K., Klarl, B.A., Myssina, S.,
641 Jendrossek, V., Ishii, S., Shimizu, T., Waidmann, M., et al. (2005). Stimulation of
642 erythrocyte ceramide formation by platelet-activating factor. *J. Cell Sci.* *118*, 1233–
643 1243.
- 644 49. Ju, X., Silveira, P.A., Hsu, W.-H., Elgundi, Z., Alingcastre, R., Verma, N.D.,
645 Fromm, P.D., Hsu, J.L., Bryant, C., Li, Z., et al. (2016). The Analysis of CD83
646 Expression on Human Immune Cells Identifies a Unique CD83 + -Activated T Cell
647 Population. *J. Immunol.* *197*, 4613–4625.
- 648 50. Maceyka, M., and Spiegel, S. (2014). Sphingolipid metabolites in inflammatory
649 disease. *Nature* *510*, 58–67.
- 650 51. Hannun, Y.A., and Obeid, L.M. (2008). Principles of bioactive lipid signalling:
651 lessons from sphingolipids. *Nat. Rev. Mol. Cell Biol.* *9*, 139–150.
- 652 52. Hilvo, M., Salonurmi, T., Havulinna, A.S., Kauhanen, D., Pedersen, E.R., Tell,
653 G.S., Meyer, K., Teeriniemi, A.M., Laatikainen, T., Jousilahti, P., et al. (2018).

- 654 Ceramide stearic to palmitic acid ratio predicts incident diabetes. *Diabetologia* *61*,
655 1424–1434.
- 656 53. Wang, D.D., Toledo, E., Hruby, A., Rosner, B.A., Willett, W.C., Sun, Q.,
657 Razquin, C., Zheng, Y., Ruiz-Canela, M., Guasch-Ferré, M., et al. (2017). Plasma
658 ceramides, mediterranean diet, and incident cardiovascular disease in the PREDIMED
659 trial. *Circulation* *135*, 2028–2040.
- 660 54. Lopez, X., Goldfine, A.B., Holland, W.L., Gordillo, R., and Scherer, P.E. (2013).
661 Plasma ceramides are elevated in female children and adolescents with type 2
662 diabetes. *J. Pediatr. Endocrinol. Metab.* *26*, 995–998.
- 663 55. Jensen, P.N., Fretts, A.M., Yu, C., Hoofnagle, A.N., Umans, J.G., Howard, B. V.,
664 Sitlani, C.M., Siscovick, D.S., King, I.B., Sotoodehnia, N., et al. (2019). Circulating
665 sphingolipids, fasting glucose, and impaired fasting glucose: The Strong Heart Family
666 Study. *EBioMedicine* *41*, 44–49.
- 667 56. Lemaitre, R.N., Yu, C., Hoofnagle, A., Hari, N., Jensen, P., Fretts, A.M., Umans,
668 J.G., Howard, B. V., Sitlani, C.M., Siscovick, D.S., et al. (2018). Circulating
669 sphingolipids, insulin, HOMA-IR and HOMA-B: The Strong Heart Family Study
670 Running title: Sphingolipids and insulin resistance markers. *Diabetes* *67*, 1663–1672.
- 671 57. Yu, J., Pan, W., Shi, R., Yang, T., Li, Y., Yu, G., Bai, Y., Schuchman, E.H., He,
672 X., and Zhang, G. (2015). Ceramide Is Upregulated and Associated With Mortality in
673 Patients With Chronic Heart Failure. *Can. J. Cardiol.* *31*, 357–363.
- 674 58. de Carvalho, L.P., Tan, S.H., Ow, G.S., Tang, Z., Ching, J., Kovalik, J.P., Poh,
675 S.C., Chin, C.T., Richards, A.M., Martinez, E.C., et al. (2018). Plasma Ceramides as
676 Prognostic Biomarkers and Their Arterial and Myocardial Tissue Correlates in Acute
677 Myocardial Infarction. *JACC Basic to Transl. Sci.* *3*, 163–175.
- 678 59. Pan, W., Yu, J., Shi, R., Yan, L., Yang, T., Li, Y., Zhang, Z., Yu, G., Bai, Y.,

679 Schuchman, E.H., et al. (2014). Elevation of ceramide and activation of secretory acid
680 sphingomyelinase in patients with acute coronary syndromes. *Coron. Artery Dis.* 25,
681 230–235.

682 60. Bergman, B.C., Brozinick, J.T., Strauss, A., Bacon, S., Kerege, A., Bui, H.H.,
683 Sanders, P., Siddall, P., Kuo, M.S., and Perreault, L. (2015). Serum sphingolipids:
684 relationships to insulin sensitivity and changes with exercise in humans. *Am. J.*
685 *Physiol. Endocrinol. Metab.* 309, 398–408.

686 61. Hinterwirth, H., Stegemann, C., and Mayr, M. (2014). Lipidomics: Quest for
687 molecular lipid biomarkers in cardiovascular disease. *Circ. Cardiovasc. Genet.* 7,
688 941–954.

689

Figure Legends

Figure 1: Schematic overview of the biosynthetic pathways for (A) *N*-acyl ethanolamines and (B) ceramides

A) *N*-acyl ethanolamine species (NAE), including the endocannabinoid anandamide (AEA), are produced through four independent enzymatic pathways from the membrane phospholipid precursor (*N*-acyl phosphatidylethanolamine; NAPE). Fatty acid amide hydrolase (*FAAH*) degrades NAEs to free fatty acids (such as arachidonic acid for AEA) and ethanolamine. NAEs have signalling roles in pain, obesity, inflammation, and neurotransmission.

B) Ceramide (CER) species are biosynthesised via the enzyme serine palmitoyltransferase (*SPTLC1-3*) that converts palmitoyl-CoA and L-serine to 3-keto dihydrosphingosine, in the rate-limiting step of the sphingolipid *de novo* pathway. The resulting dihydrosphingosine (C18DS) is coupled to various fatty acids via ceramide synthases (CERS) to generate dihydroceramides [CER[NDS]] that are further converted to CER[NS] via the enzyme delta 4-desaturase (*DEGSI*). Conversion of these pro-apoptotic CER[NS] species to sphingosine (C18S) and sphingosine 1-phosphate (C18S1P), with roles in cell survival, degrades ceramides through reversible reactions. CER[NS] are also reversibly converted to sphingomyelin (SM) or further metabolised to ceramide 1-phosphate [C1P]). In a similar way, addition of alpha-hydroxy fatty acids to C18DS, results in CER[ADS] species.

Measured lipid species are in bold; genes encoding enzymes are in italics; genes identified through SNPs that associated at GWAS with circulating lipid levels are in red.

Figure 2: Heritability estimates of *N*-acyl ethanolamines and ceramides found in human plasma.

This figure depicts the heritability estimated for each lipid species using SNP-based GCTA software (y-axis) and reported pedigree-based QTDT software (x-axis). This data is presented in detail in Table S5.

Figure 3: Family-based GWAS results for *N*-acyl ethanolamines and the lead SNP in fatty acid amide hydrolase (*FAAH*).

The radar plot depicts the P-value for association between the lead SNP and eQTL of *FAAH* (rs324420) and each NAE species. The P-values were grouped into “ $<5 \times 10^{-8}$ ” ($P < 5 \times 10^{-8}$, outermost ring), “ $\times 10^{-6}$ ” ($P = 5.0 \times 10^{-8} - 9.9 \times 10^{-6}$ [of which there are no NAE species]), “ $\times 10^{-5}$ ” ($1.0 \times 10^{-5} - 9.9 \times 10^{-5}$), and “NS” (not significant) at the center of the radar.

Figure 4: LocusZoom plot of the association of PEA with *FAAH* SNP rs324420

The LocusZoom plot depicts the association of *N*-acyl ethanolamine lipid species PEA with *FAAH* SNP rs324420 on chromosome 1. The r^2 for each SNP is depicted in colour. The plot was created using the LocusZoom plot tools at <http://locuszoom.sph.umich.edu/>.

Figure 5: Family-based GWAS results for CER[NS] and precursor CER[NDS] with an exemplar SNP in serine palmitoyltransferase (*SPTLC3*).

The radar plot depicts the P-value for association between the lead SNP and liver eQTL of *SPTLC3* (rs680379) with CER species. The P-values were grouped into “ $<5 \times 10^{-8}$ ” ($P < 5 \times 10^{-8}$, outermost ring), “ $\times 10^{-6}$ ” ($P = 5.0 \times 10^{-8} - 9.9 \times 10^{-6}$), “ $\times 10^{-5}$ ” ($1.0 \times 10^{-5} - 9.9 \times 10^{-5}$), and “NS” (not significant) at the center of the radar.

Figure 6: LocusZoom plot of the association of CER[N(24)S(19)] with *SPTLC3* SNP rs680379

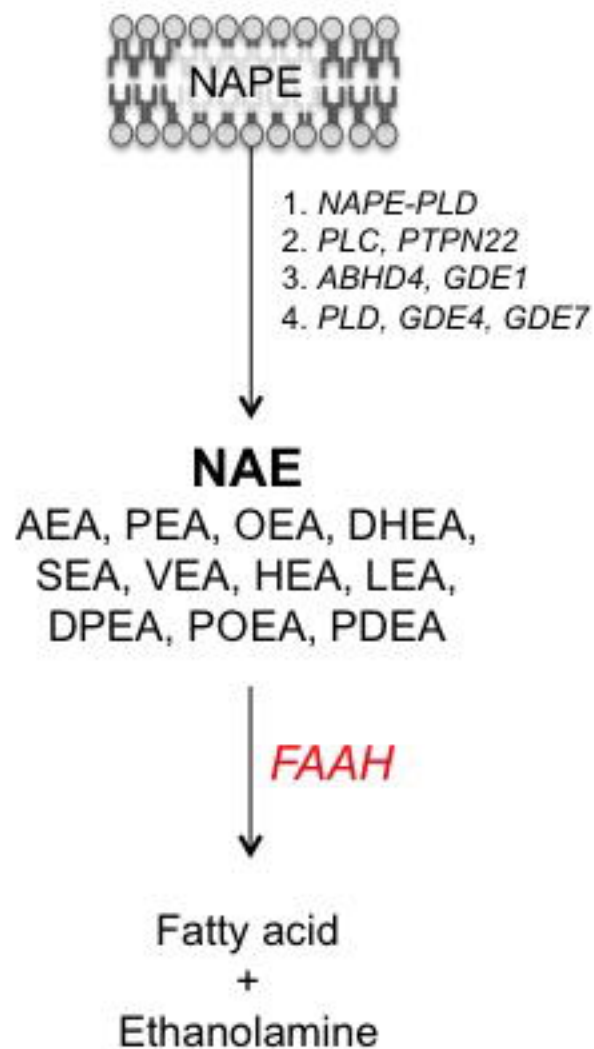
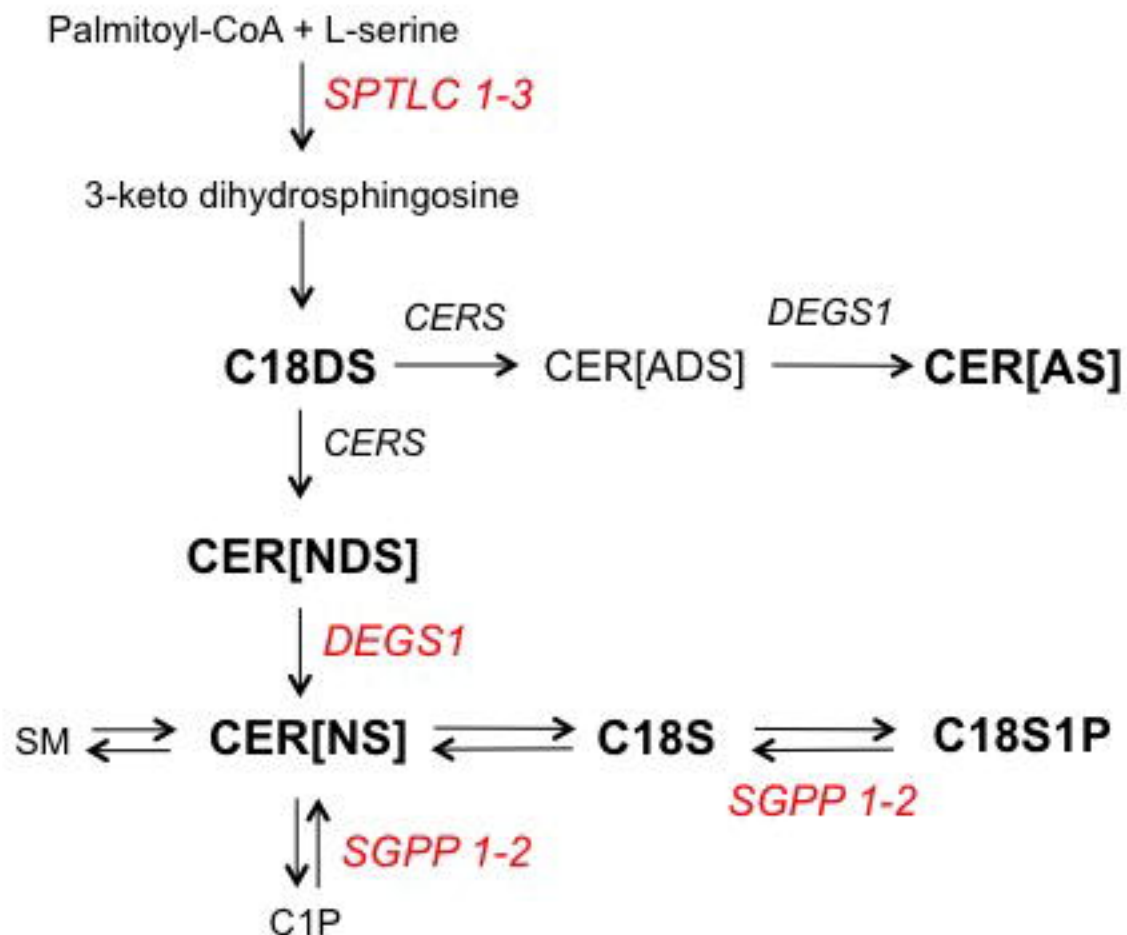
The LocusZoom plot depicts the association of CER[N(24)S(19)] with *FAAH* SNP rs680379 on chromosome 1. While there is a group of lead SNPs, this SNP was depicted as it has been identified previously to associate at GWAS with sphingolipid species. The r^2 for each SNP is depicted in colour. The plot was created using the LocusZoom plot tools at <http://locuszoom.sph.umich.edu/>.

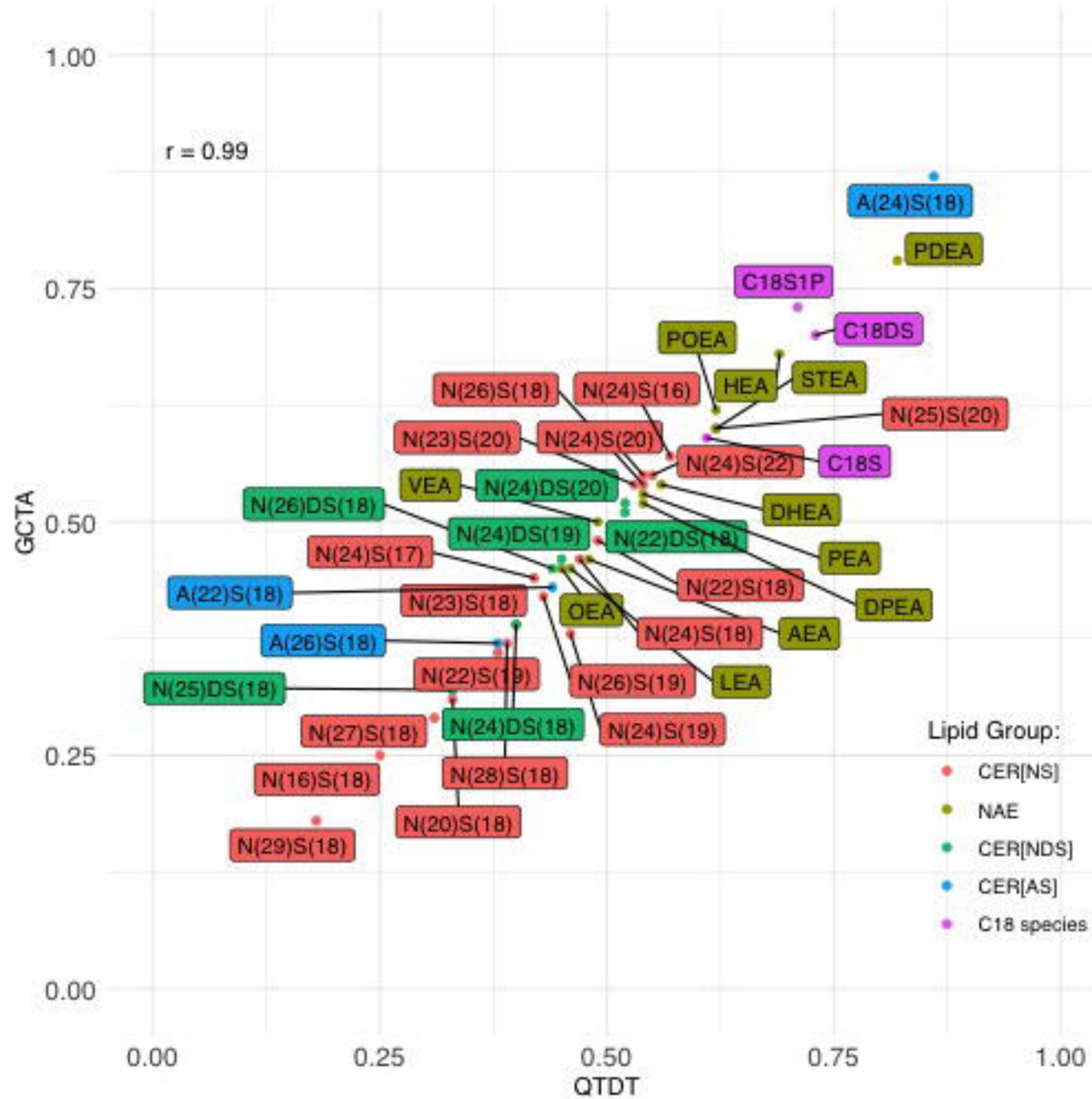
Tables

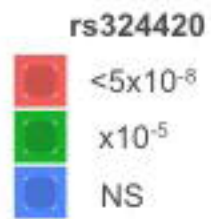
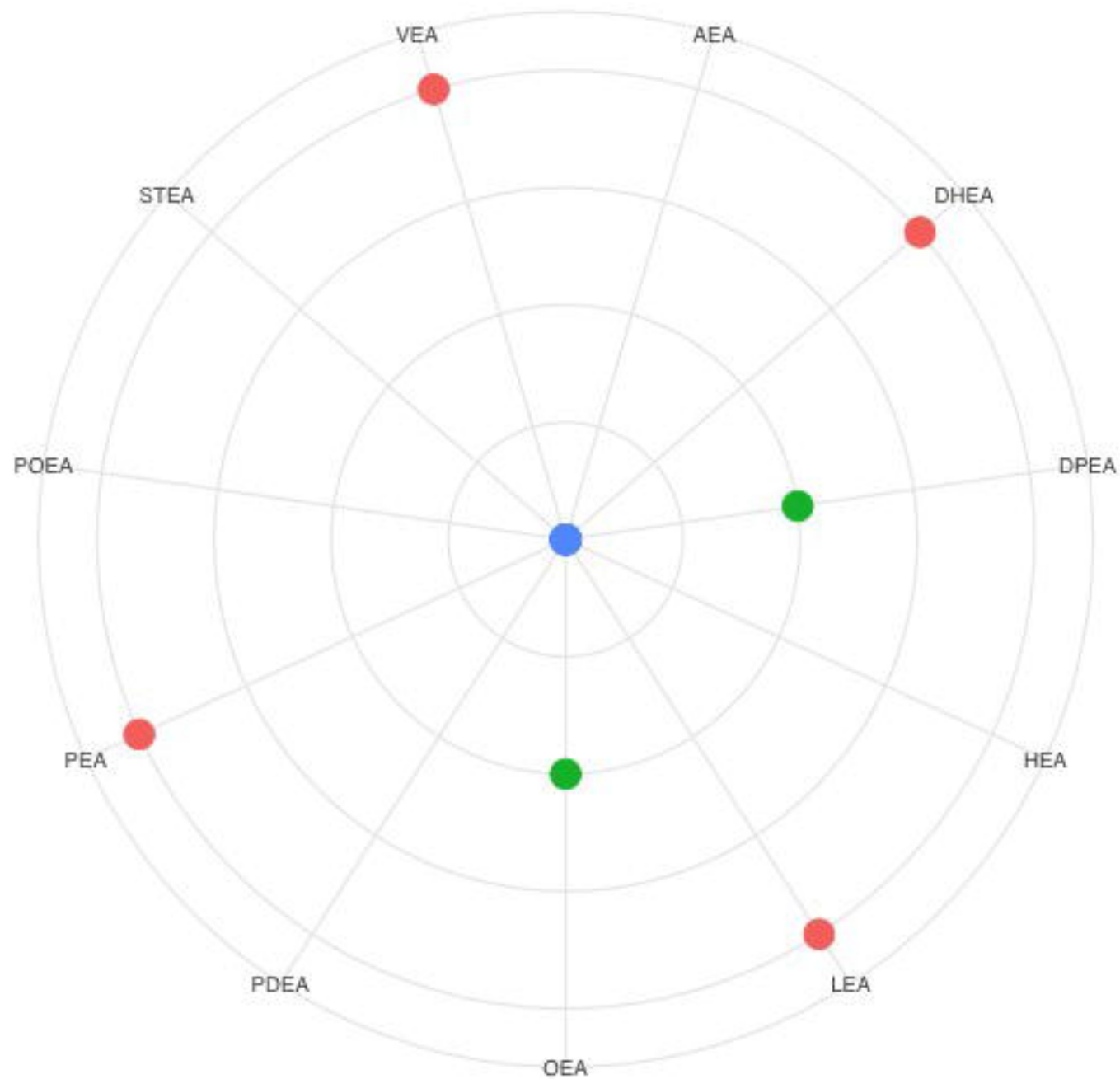
Table 1: Summary statistics for the study participants.

Data is shown as mean and standard deviation (SD) unless otherwise indicated; BMI, body mass index; WHR, waist-hip ratio.

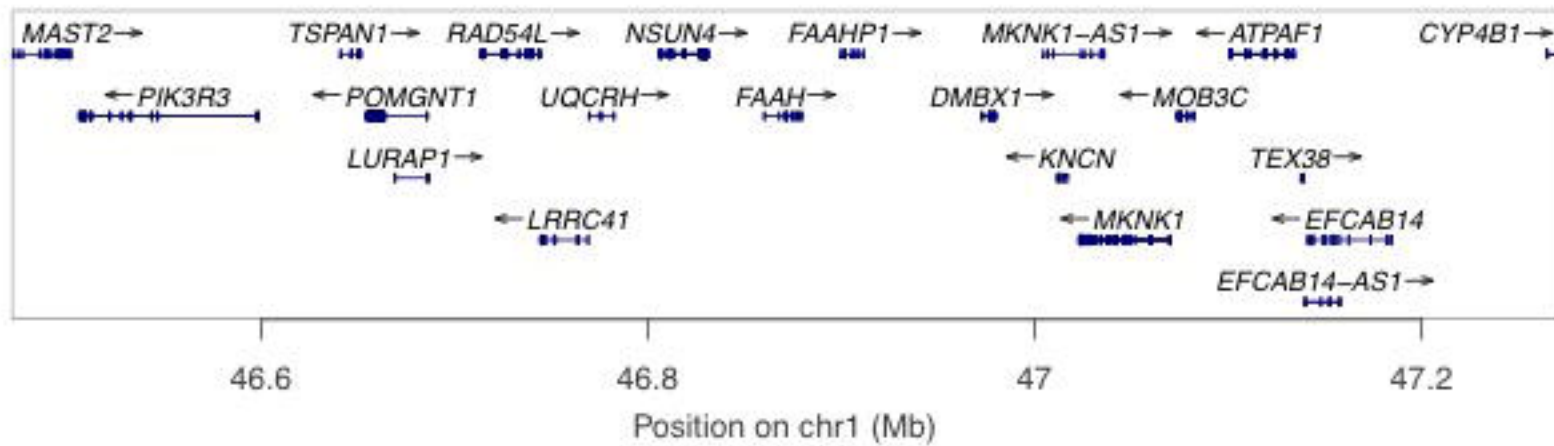
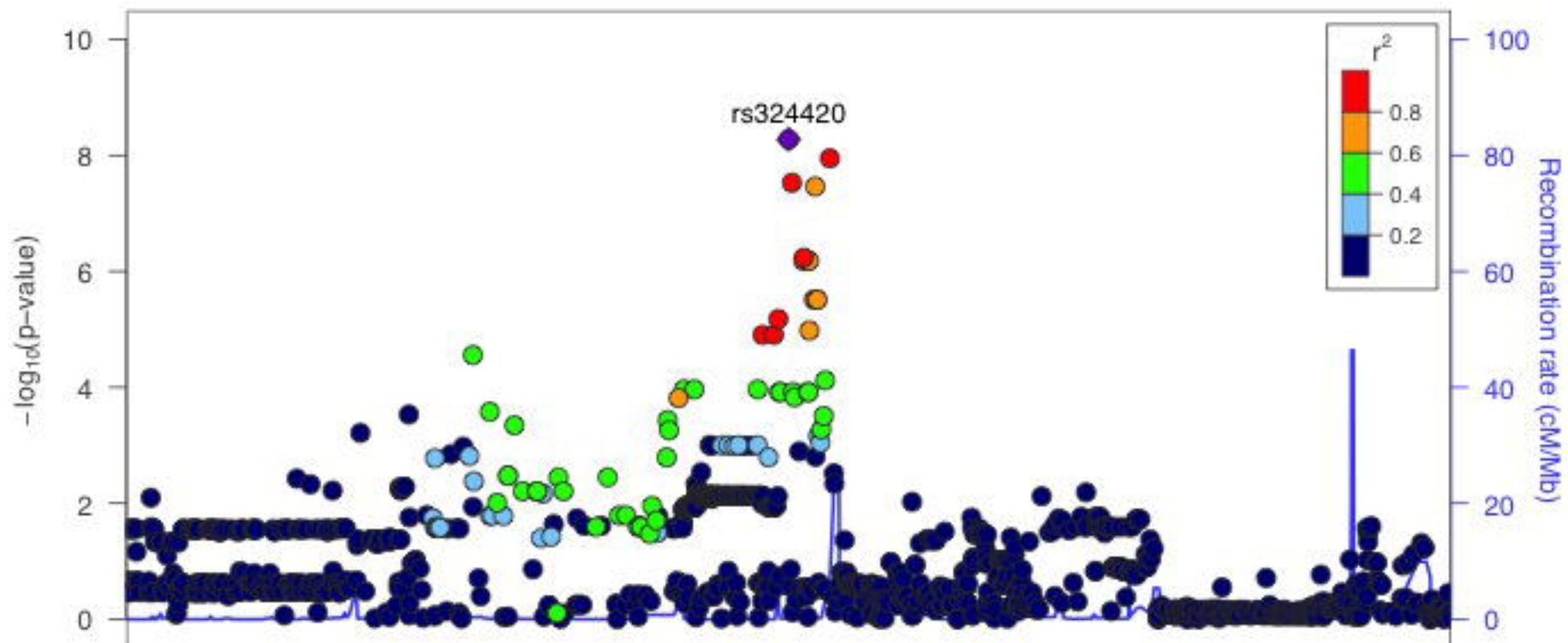
Trait	Mean (SD)
Gender	47% Male
Hypertensive	33%
Mean Blood Pressure	138/83 mmHg
Age (years)	49 (15)
BMI	26.04 (4.33)
WHR	0.86 (0.09)
Cholesterol (mmol/L)	5.61 (1.20)

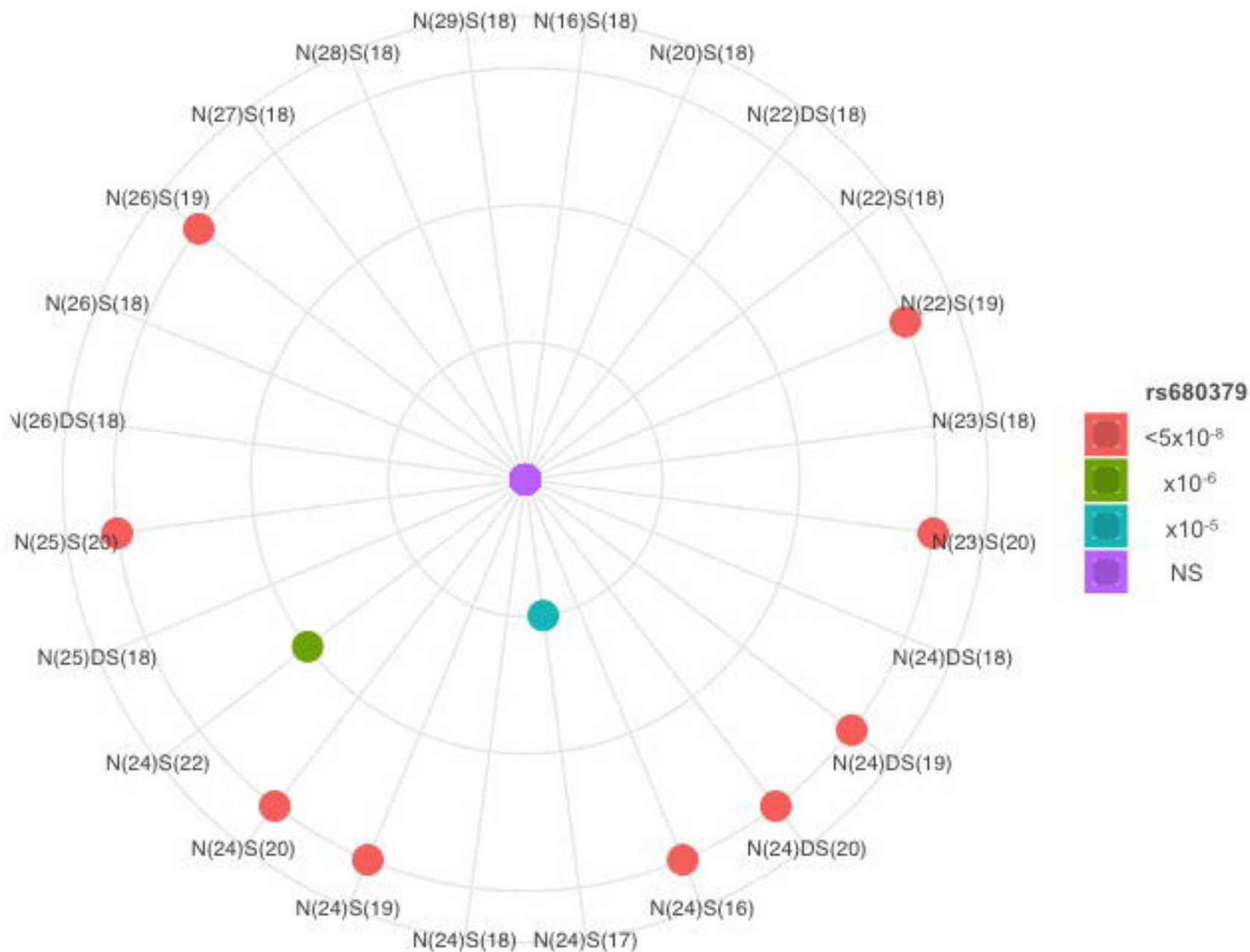
A**B**





Plotted SNPs





Plotted SNPs

